Repeat E anchors Xist RNA to the inactive X chromosomal compartment through CDKN1A-interacting protein (CIZ1)

Hongjae Sunwoo[a,b,c], David Colognori[a,b,c], John E. Froberg[a,b,c], Yesu Jeon[a,b,c], and Jeannie T. Lee[a,b,c,1]

[a]Howard Hughes Medical Institute, Massachusetts General Hospital, Boston, MA 02114; [b]Department of Molecular Biology, Massachusetts General Hospital, Boston, MA 02114; and [c]Department of Genetics, Harvard Medical School, Boston, MA 02115

Contributed by Jeannie T. Lee, August 20, 2017 (sent for review June 21, 2017; reviewed by Montserrat C. Anguera and J. Mauro Calabrese)

X chromosome inactivation is an epigenetic dosage compensation mechanism in female mammals driven by the long noncoding RNA, Xist. Although recent genomic and proteomic approaches have provided a more global view of Xist's function, how Xist RNA localizes to the inactive X chromosome (Xi) and spreads in cis remains unclear. Here, we report that the CDKN1-interacting zinc finger protein CIZ1 is critical for localization of Xist RNA to the Xi chromosome territory. Stochastic optical reconstruction microscopy (STORM) shows a tight association of CIZ1 with Xist RNA at the single-molecule level. CIZ1 interacts with a specific region within Xist exon 7–namely, the highly repetitive Repeat E motif. Using genetic analysis, we show that loss of CIZ1 or deletion of Repeat E in female cells phenocopies one another in causing Xist RNA to delocalize from the Xi and disperse into the nucleoplasm. Interestingly, this interaction is exquisitely sensitive to CIZ1 levels, as overexpression of CIZ1 likewise results in Xist delocalization. As a consequence, this delocalization is accompanied by a decrease in H3K27me3 on the Xi. Our data reveal that CIZ1 plays a major role in ensuring stable association of Xist RNA within the Xi territory.

Xist | X inactivation | Repeat E | CIZ1 | noncoding RNA

X chromosome inactivation (XCI) is one of the most extensively studied epigenetic processes to date. Since its discovery more than 50 years ago, numerous genetic and cellular studies have uncovered several RNA and protein factors to be high-confidence regulators of this process (reviewed in refs. 1–3). Recently, the advent of genomic (4–7) and proteomic (8–10) approaches for studying long noncoding RNAs has brought about a more holistic view of XCI mechanics. Still, how Xist is able to spread across only one of two X chromosomes and be retained within the inactive X (Xi) territory as an Xist cloud (11) remains one of the most challenging questions to address. Despite an intuitive perception that Xist localization must be confined in cis to the allele from which it is transcribed, specific molecular players have yet to be fully elucidated. Although the transcription factor YY1 has been ascribed a role for the nucleation of Xist RNA in cis to the Xi (12, 13), how Xist RNA spreads exclusively along the same chromosome and remains stably associated with it is unknown. The nuclear matrix protein HNRNPU (also known as SAF-A) was also found to be important for Xist RNA localization (13, 14). However, neither protein is particularly enriched on the Xi relative to other chromosomes, and may function indirectly or in a cell-type-specific manner (15, 16).

While performing superresolution stochastic optical reconstruction microscopy (STORM) to investigate candidate protein factors for their ability to colocalize with Xist RNA (17), we came across an ASH2L antibody that piqued our interest. This Trithorax protein, usually associated with active genes, was previously reported to colocalize with Xist RNA in immunofluorescence (IF) experiments (18). Indeed, our initial analysis confirmed this colocalization, with the antibody exhibiting an exceptionally high level of colocalization with Xist RNA in mouse embryonic stem (ES) and immortalized embryonic fibroblast (MEF) cells (Fig. S1 *A* and *B*). However, further analysis suggested ASH2L was not the recognized epitope (Figs. S1). IF showed that knockdown of ASH2L by siRNA failed to abolish the Xi-enriched signal, despite effective knockdown at both the protein and mRNA levels (Fig. S1 *C* and *D*). In addition, IF using two other commercially available antibodies or an EGFP fusion protein failed to show any sign of ASH2L enrichment on the Xi (Figs. S1*E* and S2).

To identify the epitope associated with the Xi, we performed proteomic analysis of the material immunoprecipitated by the presumptive ASH2L antibody (Table S1). To screen candidates, we constructed and transiently transfected several EGFP-fusion proteins into HEK293FT cells. Among them, CIZ1 arose as a highly enriched factor on the Xi (Fig. 1*A* and Figs. S2 and S3). CIZ1 was originally identified as a CDKN1A-interacting protein (19) and has been reported to play a role in cell cycle progression (20, 21). It can be found in tight association with the nuclear matrix and is resistant to high salt extraction (22). CIZ1 is also linked to several human diseases, including cervical dystonia (23) and lung cancer (24). Furthermore, although not previously implicated in XCI, CIZ1 did emerge as a potential Xist RNA interactor in one of the recent proteomic studies (8).

We confirmed CIZ1's localization to the Xi in several ways. First, CIZ1 colocalization with Xist RNA in female mouse cells was examined by IF, using an in-house CIZ1 antibody (Fig. 1*A* and Fig. S3), as well as by C-terminal knock-in of EGFP at the endogenous CIZ1 locus (Fig. 1*A* and Fig. S4). Importantly, Xi localization of CIZ1 was not observed in an Xist-deleted female MEF (25), indicating Xist is necessary for CIZ1 recruitment to the Xi (Fig. 1*B*). To investigate the molecular localization of CIZ1, we performed superresolution imaging analysis using STORM to

Significance

The long noncoding Xist RNA coats and silences one X chromosome in female cells. How Xist localizes in cis to the inactive X compartment is not clear. Here, we reveal a required interaction between CIZ1 protein and Xist Repeat E motifs. Stochastic optical reconstruction microscopy (STORM) shows a tight association of CIZ1 with Xist RNA at the single-molecule level. Deletion of either CIZ1 or Repeat E causes dispersal of Xist RNA throughout the nucleoplasm, as well as loss of the heterochromatin mark H3K27me3 from the inactive X chromosome. We have thus identified a critical factor for stable association of Xist RNA with the inactive X chromosome.

Author contributions: H.S. and J.T.L. designed research; H.S., D.C., and J.E.F. performed research; Y.J. contributed new reagents/analytic tools; H.S., D.C., and J.T.L. analyzed data; and H.S., D.C., and J.T.L. wrote the paper.

Reviewers: M.C.A., University of Pennsylvania; and J.M.C., University of North Carolina at Chapel Hill.

The authors declare no conflict of interest.

[1]To whom correspondence should be addressed. Email: lee@molbio.mgh.harvard.edu.

This article contains supporting information online at www.pnas.org/lookup/suppl/doi:10.1073/pnas.1711206114/-/DCSupplemental.

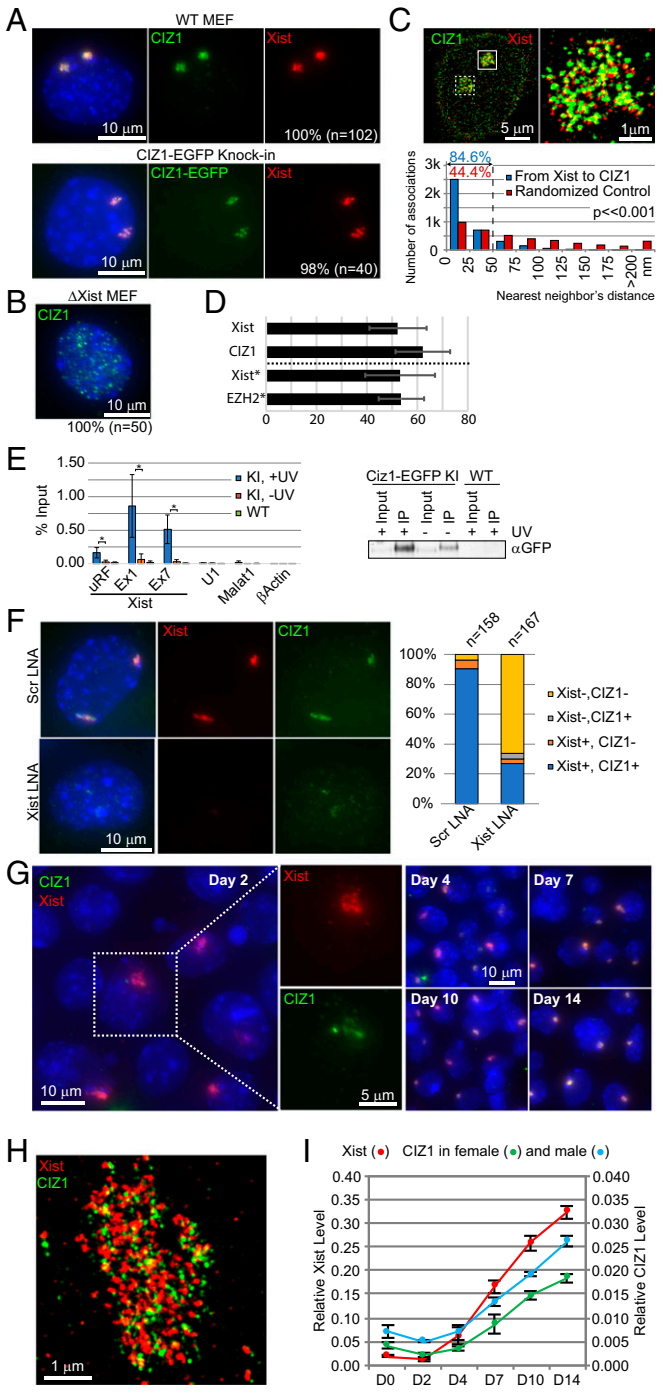

Fig. 1. CIZ1 is a Xi-localizing protein. (*A*) CIZ1 colocalizes with Xist RNA in transformed tetraploid female mouse embryonic fibroblasts (WT MEF). CIZ1-EGFP colocalizes with Xist in MEFs carrying an EGFP knock-in at the C terminus of the endogenous CIZ1 locus. (*B*) CIZ1 shows no Xi localization pattern in female MEFs with Xist deleted. (*C*) Two-color STORM image showing CIZ1 colocalization with Xist RNA in female MEF. The two Xist clouds are boxed, with one shown at higher magnification. The nearest neighbor's distance measurement shows most of CIZ1 is proximal to Xist RNA, significantly more than randomized control (*P* values from Kolmogorov-Smirnov test). (*D*) Stoichiometry of the number of Xist puncta relative to CIZ1 puncta per Xi. *Data for Xist vs. EZH2 are taken from ref. 17 for comparison purposes. Note that each punctum could have multiple molecules of protein or RNA. This analysis is strictly focused on the number of clusters (puncta) of protein or RNA. (*E*) UV-RIP using CIZ1-EGFP knock-in cell line shows CIZ1-EGFP is in close interaction with Xist RNA. Immnuoblot verifies CIZ1-EGFP was pulled down efficiently compared with 10% input. *Statistically significant difference in paired Student *t* test. (*F*) LNA knock-off of Xist RNA from the Xi also displaces CIZ1 within 1 h post transfection while scrambled control LNA (Scr) has no effect. (*G*) Xist RNA FISH and CIZ1 IF on days 2–14 of female mouse ES cell differentiation. The boxed area in day 2 was enlarged and contrast further adjusted to show weak level of CIZ1 still colocalizing with Xist at this early time. (*H*) STORM imaging of Xist RNA FISH and CIZ1 IF on the Xi in day 4 differentiating ES cell. (*I*) Quantitative RT-PCR shows CIZ1 is up-regulated along with Xist during female mouse ES cell differentiation. CIZ1 also shows similar up-regulation in male ES cells.

resolve single Xist particles that were previously deduced to contain one to two molecules of Xist RNA (17). Intriguingly, CIZ1 showed greater proximity to puncta of Xist transcripts than any other previously examined Xi-associated factor (Fig. 1*C*), including EZH2, H3K27me3, SMCHD1, H4K20me1, and HBiX1 (17). A large fraction of CIZ1-Xist pairs were within 25 nm of each other (Fig. 1*C*), a distance within the empirical resolution (20–30 nm) of STORM microscopy. Approximately 85% of all pairs showed a separation of <50 nm distance. This distance is significantly different from that which would be derived from a random model ($P << 0.001$).

These data suggested a very close relationship between CIZ1 and Xist RNA. We counted the number of Xist puncta relative to CIZ1 puncta and observed a similar stoichiometry, with 52.2 ± 11.2 for Xist and 61.9 ± 10.8 for CIZ1 (Fig. 1*D*). This similarity is consistent with a tight coclustering of Xist and CIZ1, and is also consistent with the nearly equal stoichiometry of Xist to Polycomb repressive complex 2 puncta, as previously reported (17). To probe further whether Xist and CIZ1 might associate with each other at a molecular level, we performed UV-crosslinked RNA immunoprecipitation (UV-RIP), using our CIZ1-EGFP knock-in cell line (Fig. 1*E*). A clear enrichment over non-UV-crosslinked control or the parental cell line lacking EGFP supported a potential direct interaction between CIZ1 and Xist RNA in vivo. To test this relationship further, we used locked nucleic acid (LNA) antisense oligonucleotides to "knock off" Xist RNA from the Xi (26) and asked whether there were consequences on CIZ1 localization. LNA knock-off caused an immediate delocalization of CIZ1 that was detectable as early as 20 min after transfection, in a manner that was concurrent with loss of Xist RNA (Fig. 1*F* and Fig. S5*A*). Recovery of both Xist and CIZ1 occurred very slowly after 4–8 h in a concordant fashion (Fig. S5*B*). Taken together, these data support a very close association between Xist RNA and CIZ1 in Xi localization.

We then examined the time course of CIZ1 recruitment in differentiating female ES cells: an ex vivo model for X chromosome inactivation. CIZ1 foci were observed as soon as Xist RNA was detected by RNA FISH on day 2 of differentiation, although CIZ1 foci were less intense and appeared somewhat punctate at this early point (Fig. 1*G*). Between days 4 and 14, CIZ1 signal continued to accumulate coincidentally with Xist RNA in differentiating female ES cells (Fig. 1*G*). Nearly all Xist foci showed a confidently detectable level of overlapping CIZ1 localization by day 4 (98%, $n = 117$). STORM imaging of day 4 ES cells further confirmed proximal localization of CIZ1 to Xist RNA (Fig. 1*H*). Quantitative RT-PCR demonstrated that CIZ1 levels were up-regulated during female cell differentiation with a time course that paralleled Xist's up-regulation (Fig. 1*I*). In differentiating male ES cells, CIZ1 was also transcriptionally up-regulated (Fig. 1*I*), but failed to accumulate on the single active X chromosome, consistent with the absence of XCI in male fibroblasts (Fig. S5*C*). In contrast, CIZ1 could be recruited ectopically to an induced Xist transgene in male fibroblasts (Fig. S5*D*), indicating Xist expression is sufficient for CIZ1 recruitment. We conclude that CIZ1 is rapidly recruited

CELL BIOLOGY

to the Xi during XCI, and that Xist RNA is both necessary and sufficient to recruit CIZ1.

To understand CIZ1's role during XCI, we established two female MEF cell lines harboring small deletions in CIZ1's exon 5 (present in all splicing isoforms), using the CRISPR/Cas9 system (Fig. 2 *A* and *B*). Two knockout (KO) clonal lines were established: KO1 has a frameshift deletion, whereas KO5 has a short (≤16 aa) in-frame deletion (Fig. S6*A*). Both KO cell lines showed loss of CIZ1 protein in Western blot analysis (Fig. 2*B*), suggesting the frame-shift and in-frame mutations both produced unstable protein. Intriguingly, loss of CIZ1 protein in both cell lines led to an aberrant pattern of Xist accumulation on the Xi (Fig. S7*A*). Analysis by 3D STORM superresolution imaging showed poorly localized Xist particles and a gradient of Xist concentration, indicative of diffusion away from the site of synthesis (Xi) (Fig. 2*C*). Xist RNA FISH and X chromosome paint confirmed that Xist RNA localized beyond the Xi chromosome territory (Fig. 2*D*). This aberrant localization pattern was not caused by any evident effect on Xist expression (Fig. 2*E*). Quantitative RT-PCR confirmed that CIZ1 loss did not significantly affect levels of HNRNPU, another factor critical for proper Xist localization (14) (Fig. 2*E*). We also generated CIZ1 KO female ES cells and observed a similar Xist localization defect (Figs. S6*B* and S7*B*). Significantly, the role of CIZ1 in Xist localization is conserved in human, as KO of CIZ1 in HEK293FT cells likewise resulted in dispersal of XIST RNA (Figs. S6*C* and S7*C*). Xist delocalization led to a consequent decrease or loss of H3K27me3 on the Xi in KO MEFs (Fig. 2*F*), consistent with a requirement for Xist in recruiting Polycomb repressive complex 2. Taken together, these data demonstrate that CIZ1 is required for Xist localization.

We then investigated whether specific motifs in Xist RNA are responsible for CIZ1 recruitment. We first tested female MEFs carrying Xist transgenes with various subdeletions (12). Cell lines with a wild-type Xist transgene or a transgene with a Repeat A deletion were both capable of recruiting CIZ1 (Fig. 3*A*). In contrast, a transgene containing only exon 1 of Xist failed to recruit CIZ1 (Fig. 3*B*), arguing that critical CIZ1-interacting domains lie outside of exon 1. To pinpoint required domains, we began by deleting the entire exon 7 (the largest exon after the first), using the CRISPR/Cas9 system and a pair of guide RNAs flanking the

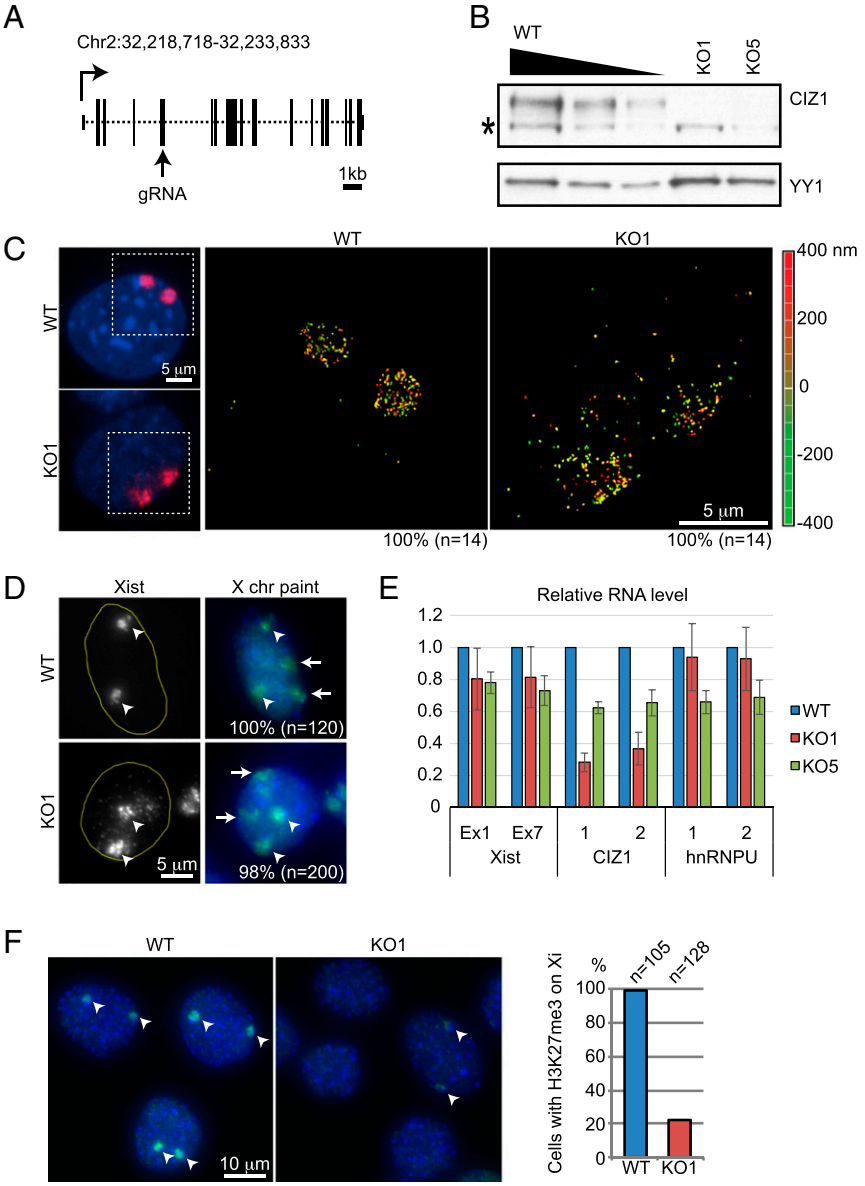

Fig. 2. CIZ1 is critical for maintenance of the Xist cloud and Xi chromatin marks. (*A*) Schematic diagram of murine CIZ1 gene structure (based on mm9 reference genome) and guide RNA target position. Arrow indicates the orientation of transcription, with boxes and dotted lines representing exons and introns, respectively. (*B*) Immunoblot confirms depletion of CIZ1 protein in KO1 and KO5 cell lines. YY1 was used as a loading control. *Nonspecific protein band. (*C*) STORM imaging of boxed areas shows Xist particles diffusing away in KO compared with tight cloud in WT cells. Depth in the *z*-plane is color-coded from red (+400 nm) to green (−400 nm). (*D*) Xist RNA in KO cells is detected outside the X chromosome territory. Arrows and arrowheads denote the two active and inactive X chromosomes, respectively. (*E*) CIZ1 depletion has minimal effect on Xist or HNRNPU RNA levels. Two primer sets were used for each gene. Mean ± SD for three replicates is shown. (*F*) H3K27me3 on the Xi is lost or reduced in a significant fraction of CIZ1 KO cells. Arrowheads indicate H3K27me3 enrichment on Xi.

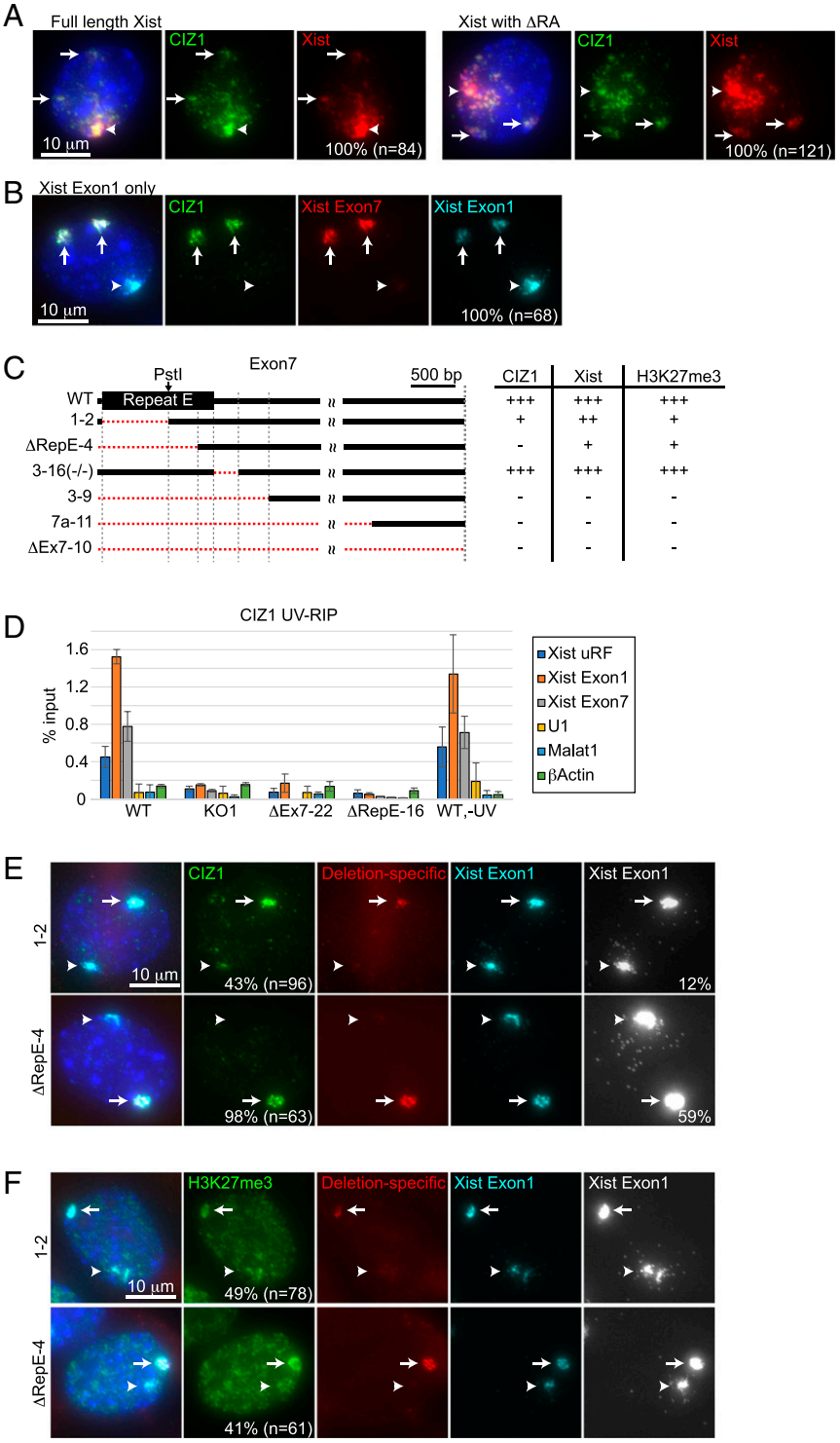

Fig. 3. CIZ1 interacts with Xist RNA through the Repeat E region. (*A*) Transgenes containing either full-length Xist or Xist lacking the Repeat A region are sufficient to recruit CIZ1. Arrows indicate Xist cloud from endogenous loci; arrowhead indicates overexpressed Xist from stably integrated transgene. (*B*) A transgene containing only Xist exon 1 is insufficient to recruit CIZ1. (*C*) Schematic diagram showing several cell lines with endogenous subdeletions within Xist exon 7. Red dotted lines denote deleted segments. Presence or absence of CIZ1 recruitment, normal Xist cloud, and H3K27me3 on Xi is indicated by "+" or "−," respectively. Only weak CIZ1 recruitment was observed in clone 1-2. At least 50 cells were counted for each genotype. (*D*) UV-RIP shows CIZ1-Xist interaction requires Repeat E within exon 7. ΔRepE-16 clone contains the entire Repeat E deleted on both Xis. Mean ± SD for three replicates is shown. (*E*) CIZ1 IF/Xist RNA FISH of representative cells shows loss of CIZ1 recruitment and dispersed Xist RNA away from the Xi in indicated deletion cell lines. Arrow indicates WT Xist; arrowhead indicates Xist with deletion. Contrast was enhanced for Xist RNA FISH to show single particles outside the main cloud. (*F*) H3K27me3 IF/Xist RNA FISH shows loss of H3K27me3 and dispersed Xist RNA away from the Xi as in *E*.

endogenous locus in MEFs (Fig. 3*C*, see "ΔEx7-10"). Because the MEFs are tetraploid with two Xis, we could isolate clones with one Xi containing the desired deletion and the other serving as an internal control within the same nucleus, as well as clones with deletions on both Xis. Deletion of the entire exon 7 not only failed to recruit CIZ1 but also phenocopied the Xist delocalization and loss of H3K27me3, as seen in CIZ1 null MEFs (Fig. 3*C* and Figs. S8 and S9, see "ΔEx7-10"). This phenotype contrasted sharply with that of wild-type Xist RNA in the same nucleus of each KO cell. UV-RIP-qPCR showed that Xist ΔEx7-22 (containing the same deletion as ΔEx7-10, but on both Xis) could no longer be pulled down by CIZ1 protein (Fig. 3*D*). Likewise, enrichment of H3K27me3 was lost on both Xis (Fig. 3C and Figs. S8 and S9). Thus, exon 7 of Xist RNA is critical for CIZ1 recruitment to the Xi.

Within exon 7 lies one of Xist's many repetitive motifs, Repeat E. Deleting this entire 1.2-kb Repeat E motif resulted in complete loss of CIZ1 and near-complete loss of H3K27me3 IF signal from the Xi, along with severe disruption of the Xist cloud (Fig. 3*C* and Figs. S8 and S9, see "3-9" and "7a-11"). Finer mapping revealed that deleting the first 800 nucleotides

CELL BIOLOGY

(containing the highly repetitive sequences upstream of a PstI restriction site) was enough to ablate CIZ1 and H3K27me3 IF signal in 50% of the population, along with some disruption of the Xist cloud (Fig. 3 *C*, *E*, and *F*, see "1-2"). A larger deletion encompassing the first 1 kb of Repeat E further reduced CIZ1 IF signal below detection in nearly all cells. This was accompanied by an increased disruption of the Xist cloud and similar loss of H3K27me3 in 50% of cells (Fig. 3 *C*, *E*, and *F*, see "ΔRepE-4"). In general, the larger the deletion of Repeat E (beginning at the proximal end), the more pronounced effect on CIZ1/Xist localization and H3K27me3 deposition (Fig. 3*C* and Figs. S8 and S9). In addition, UV-RIP-qPCR showed that Xist ΔRepE-16 (containing the same deletion as ΔRepE-4, but on both Xis) could no longer be pulled down by CIZ1 protein (Fig. 3*D*). These data identify the Repeat E in exon 7 of Xist RNA as essential for the recruitment of CIZ1 to the Xi.

HNRNPU had been previously shown to be important as a nuclear matrix factor for the localization of Xist RNA to the Xi chromosomal territory (13, 14). Unlike CIZ1, however, HNRNPU is not seen enriched on the Xi, and may therefore function indirectly as a nuclear matrix factor for the anchorage of heterochromatic factors of various chromosomes. We asked whether CIZ1 and HNRNPU may function together in the same pathway, albeit with CIZ1 being Xi-specific and HNRNPU being more general. To test this, we generated HNRNPU KO cells using CRISPR/Cas9 (Fig. S6*C*). Surprisingly, HNRNPU KO cells were viable and exhibited two noticeable defects: slow growth and dispersed Xist clouds, consistent with previous experiments using HNRNPU siRNA knockdown (14). Interestingly, CIZ1 IF of HNRNPU KO cells revealed that CIZ1 remained colocalized with Xist RNA, despite Xist particles being dispersed throughout the nucleoplasm (Fig. 4*A*), with a Pearson's coefficient of >0.8. Fluorescence intensity showed CIZ1 and Xist signals peaked together nearly perfectly along a linear 8-μm distance, and this tight association was evident by STORM imaging of the same nuclei (Fig. 4*A*). Thus, CIZ1 interacts with Xist RNA independent of HNRNPU. HNRNPU UV-RIP in CIZ1 KO1 cells demonstrated that, reciprocally, HNRNPU interacts with Xist independent of CIZ1 or Xist exon 7 (Fig. 4*B*). Taken together, these data argue that both CIZ1 and HNRNPU are necessary for Xist localization to the Xi. However, their interactions with Xist RNA occur independent of each other.

Maintaining physiological levels of CIZ1 seems crucial. Intriguingly, although transient overexpression of EGFP alone did not influence Xist localization, overexpression of EGFP-CIZ1 triggered a phenotype similar to that of CIZ1 depletion (Fig. 4*C*) without changing Xist or HNRNPU levels (Fig. 4*D*). We arrived at this conclusion through assessment of the number of delocalized Xist puncta relative to controls. The assessment was performed by two independent scorers (H.S. and D.C.) and by single-blind scoring (H.S.), each yielding similar trends: ~90% of CIZ1

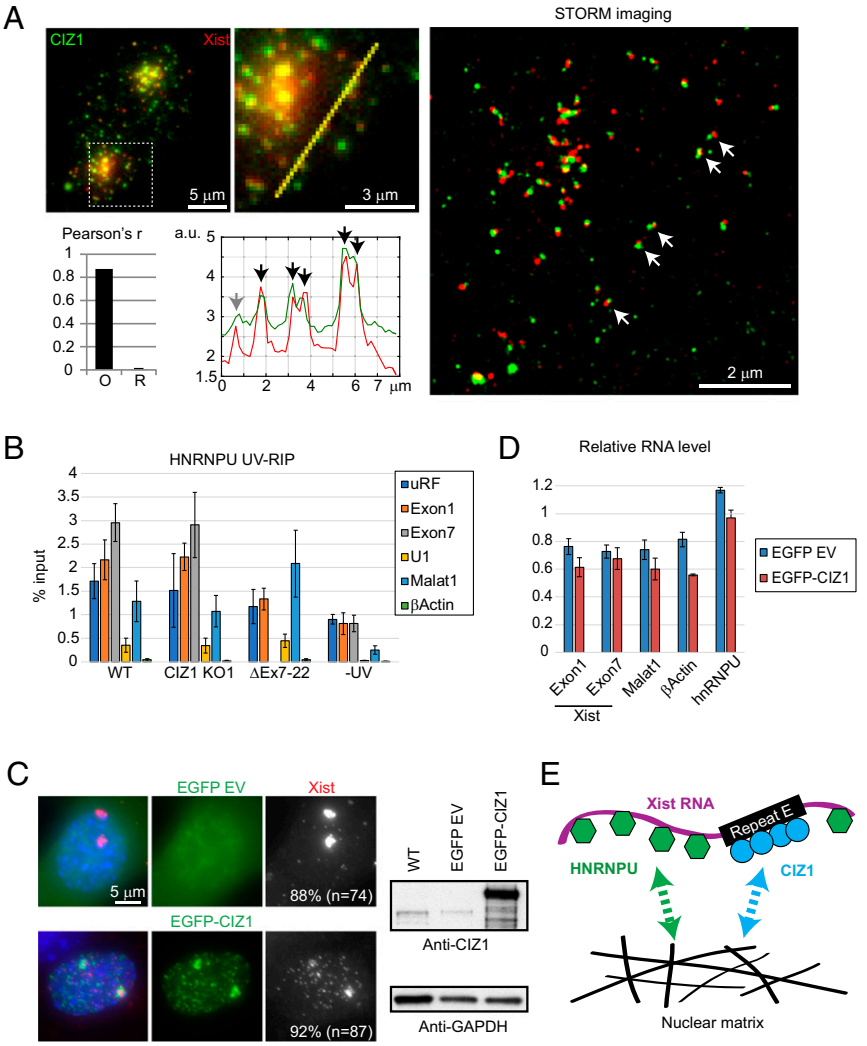

Fig. 4. CIZ1 interacts with Xist RNA independent of HNRNPU. (*A*) CIZ1 remains colocalized with Xist RNA in HNRNPU KO cells. Boxed area is enlarged. Pearson coefficient was calculated (O) along with randomized control (R) from the conventional image. Line chart of fluorescence intensity along the yellow line shows CIZ1 signal peaks together with Xist RNA signal (arrows). Two-color STORM image of the same cell shows CIZ1 colocalizes with Xist at the molecular level. Five of 6 colocalizations (black arrows in intensity chart, white arrows in STORM image) were confirmed whereas 1/6 was not seen (gray arrow). (*B*) HNRNPU UV-RIP using CIZ1 KO and Xist ΔEx7 cell lines suggests HNRNPU can interact with Xist RNA independently of CIZ1. Mean ± SD for three replicates is shown. (*C*) Overexpression of EGFP-CIZ1 phenocopies CIZ1 KO of dispersed Xist particles away from the Xi, whereas EGPF alone (EGFP EV) has no effect. Immunoblot confirms EGFP-CIZ1 overexpression compared with endogenous levels. (*D*) Overexpression of EGFP-CIZ1 does not affect Xist or HNRNPU levels. Relative RNA level is normalized to untransfected cells. Mean ± SD for three replicates is shown. (*E*) Proper Xist localization simultaneously requires at least two independent protein factors, CIZ1 and HNRNPU.

overexpressed nuclei showed disperse Xist puncta, whereas <12% of wild-type nuclei showed this pattern (Fig. 4*C*). Thus, anchorage of Xist RNA to the nuclear matrix appears to depend on a fine stoichiometric balance between Repeat E and CIZ1, with too much CIZ1 possibly saturating binding sites in the nuclear matrix and thereby preventing the anchorage of Xist Repeat E. In sum, we suggest that, although both CIZ1 and HNRNPU are required for Xist RNA localization to the Xi territory, they interact with Xist independent of each other (Fig. 4*E*).

Although much recent attention has been focused on Xist-interacting proteins that are required for transcriptional repression (2, 4, 8–10, 27–29), protein factors responsible for Xist localization have been more difficult to identify. Two previous studies, however, did report Xist exon 7 as an important domain for the spreading and localization process (30, 31). Our present study agrees with the published work on the importance of exon 7 and further identified Repeat E as a critical motif within exon 7. The function of Repeat E has also been analyzed in a recent study of XCI during female ES cell differentiation (32). While our manuscript was in preparation, CIZ1 was also identified by another group as being critical for Xist localization (33). Although there is general agreement on the role of CIZ1, several findings distinguish our study from theirs. For one, whereas our deletional analysis pinpoints the proximal half of Repeat E as being more essential for CIZ1 interaction, Ridings-Figueroa et al. (33) observed that CIZ1 is recruited primarily through the distal half of Repeat E. One possible cause of this difference could be use of inducible Xist deletion transgenes versus endogenous Xist deletions. Regardless, our study furthermore suggests a direct interaction between CIZ1 and Repeat E in vivo, using UV-RIP. This interaction is apparently also critical for the downstream deposition of the H3K27me3 repressive mark on Xi chromatin through Xist being properly localized. The intensity of IF signals and EGFP signals in the CIZ1-EGFP knock-in cell line suggests that although the number of Xist and CIZ1 clusters (puncta) is similar on the Xi (Fig. 1*D*), the actual molecular stoichiometry of CIZ1 to Xist may exceed one-to-one, with the highly repetitive nature of Repeat E enabling multiple CIZ1 proteins to bind a single Xist transcript. Repeat E is unique to Xist RNA and may provide a high-avidity platform for CIZ1 binding that would be found nowhere else in the transcriptome. A recent study of Xist secondary structure in vivo versus ex vivo showed that the Repeat E region's accessibility is highly altered in the cellular environment (34), supporting our idea of superstoichiometric binding of CIZ1 protein to this region of Xist RNA in vivo. It may be surprising that CIZ1 mutant mice are viable; however, they have a predisposition toward lymphoproliferative disorders (33, 35), consistent with a loss of Xist function and XCI in blood cells (13, 36). Future work will be directed at a molecular understanding of how CIZ1-mediated Xist localization affects the Xi heterochromatin and gene expression state.

Materials and Methods

Details are found in *SI Materials and Methods*, which includes detailed methods for cell culture, identification of CIZ1, generation of CIZ1 antibody, Xist oligo preparation, RNA FISH, X chromosome paint, immunofluorescence, microscopy, STORM imaging and analysis, antibodies, LNA transfection, UV-RIP, and generation of knock-in and KO cell lines using CRISPR/Cas9 (37, 38).

ACKNOWLEDGMENTS. We thank all members of the J.T.L. laboratory for critical comments and stimulating discussions. We also thank D. Spector (Cold Spring Harbor Laboratory) for EGFP plasmids and M. Blower (Department of Molecular Biology, Massachusetts General Hospital) for advice regarding antibody generation. H.S. was supported by the MGH ECOR Fund for Medical Discovery and J.T.L. by NIH Grant R01-GM090278. J.T.L. is an investigator of the Howard Hughes Medical Institute.

1. Lee JT (2011) Gracefully ageing at 50, X-chromosome inactivation becomes a paradigm for RNA and chromatin control. *Nat Rev Mol Cell Biol* 12:815–826.
2. Wutz A (2011) RNA-mediated silencing mechanisms in mammalian cells. *Prog Mol Biol Transl Sci* 101:351–376.
3. Disteche CM (2012) Dosage compensation of the sex chromosomes. *Annu Rev Genet* 46:537–560.
4. Calabrese JM, et al. (2012) Site-specific silencing of regulatory elements as a mechanism of X inactivation. *Cell* 151:951–963.
5. Engreitz JM, et al. (2013) The Xist lncRNA exploits three-dimensional genome architecture to spread across the X chromosome. *Science* 341:1237973.
6. Pinter SF, et al. (2012) Spreading of X chromosome inactivation via a hierarchy of defined Polycomb stations. *Genome Res* 22:1864–1876.
7. Simon MD, et al. (2013) High-resolution Xist binding maps reveal two-step spreading during X-chromosome inactivation. *Nature* 504:465–469.
8. Chu C, et al. (2015) Systematic discovery of Xist RNA binding proteins. *Cell* 161:404–416.
9. McHugh CA, et al. (2015) The Xist lncRNA interacts directly with SHARP to silence transcription through HDAC3. *Nature* 521:232–236.
10. Minajigi A, et al. (June 18, 2015) Chromosomes. A comprehensive Xist interactome reveals cohesin repulsion and an RNA-directed chromosome conformation. *Science*, 10.1126/science.aab2276.
11. Clemson CM, McNeil JA, Willard HF, Lawrence JB (1996) XIST RNA paints the inactive X chromosome at interphase: Evidence for a novel RNA involved in nuclear/chromosome structure. *J Cell Biol* 132:259–275.
12. Jeon Y, Lee JT (2011) YY1 tethers Xist RNA to the inactive X nucleation center. *Cell* 146:119–133.
13. Wang J, et al. (2016) Unusual maintenance of X chromosome inactivation predisposes female lymphocytes for increased expression from the inactive X. *Proc Natl Acad Sci USA* 113:E2029–E2038.
14. Hasegawa Y, et al. (2010) The matrix protein hnRNP U is required for chromosomal localization of Xist RNA. *Dev Cell* 19:469–476.
15. Kolpa HJ, Fackelmayer FO, Lawrence JB (2016) SAF-A requirement in anchoring XIST RNA to chromatin varies in transformed and primary cells. *Dev Cell* 39:9–10.
16. Sakaguchi T, et al. (2016) Control of chromosomal localization of Xist by hnRNP U family molecules. *Dev Cell* 39:11–12.
17. Sunwoo H, Wu JY, Lee JT (2015) The Xist RNA-PRC2 complex at 20-nm resolution reveals a low Xist stoichiometry and suggests a hit-and-run mechanism in mouse cells. *Proc Natl Acad Sci USA* 112:E4216–E4225.
18. Pullirsch D, et al. (2010) The Trithorax group protein Ash2l and Saf-A are recruited to the inactive X chromosome at the onset of stable X inactivation. *Development* 137:935–943.
19. Mitsui K, Matsumoto A, Ohtsuka S, Ohtsubo M, Yoshimura A (1999) Cloning and characterization of a novel p21(Cip1/Waf1)-interacting zinc finger protein, ciz1. *Biochem Biophys Res Commun* 264:457–464.
20. Copeland NA, Sercombe HE, Wilson RH, Coverley D (2015) Cyclin-A-CDK2-mediated phosphorylation of CIZ1 blocks replisome formation and initiation of mammalian DNA replication. *J Cell Sci* 128:1518–1527.
21. Coverley D, Marr J, Ainscough J (2005) Ciz1 promotes mammalian DNA replication. *J Cell Sci* 118:101–112.
22. Ainscough JF, et al. (2007) C-terminal domains deliver the DNA replication factor Ciz1 to the nuclear matrix. *J Cell Sci* 120:115–124.
23. Xiao J, et al. (2012) Mutations in CIZ1 cause adult onset primary cervical dystonia. *Ann Neurol* 71:458–469.
24. Higgins G, et al. (2012) Variant Ciz1 is a circulating biomarker for early-stage lung cancer. *Proc Natl Acad Sci USA* 109:E3128–E3135.
25. Zhang LF, Huynh KD, Lee JT (2007) Perinucleolar targeting of the inactive X during S phase: Evidence for a role in the maintenance of silencing. *Cell* 129:693–706.
26. Sarma K, Levasseur P, Aristarkhov A, Lee JT (2010) Locked nucleic acids (LNAs) reveal sequence requirements and kinetics of Xist RNA localization to the X chromosome. *Proc Natl Acad Sci USA* 107:22196–22201.
27. Zhao J, Sun BK, Erwin JA, Song JJ, Lee JT (2008) Polycomb proteins targeted by a short repeat RNA to the mouse X chromosome. *Science* 322:750–756.
28. Plath K, et al. (2003) Role of histone H3 lysine 27 methylation in X inactivation. *Science* 300:131–135.
29. Wang J, et al. (2001) Imprinted X inactivation maintained by a mouse Polycomb group gene. *Nat Genet* 28:371–375.
30. Chow JC, et al. (2007) Inducible XIST-dependent X-chromosome inactivation in human somatic cells is reversible. *Proc Natl Acad Sci USA* 104:10104–10109.
31. Yamada N, et al. (2015) Xist exon 7 contributes to the stable localization of Xist RNA on the inactive X-chromosome. *PLoS Genet* 11:e1005430.
32. Yue M, et al. (2017) Xist RNA repeat E is essential for ASH2L recruitment to the inactive X and regulates histone modifications and escape gene expression. *PLoS Genet* 13:e1006890.
33. Ridings-Figueroa R, et al. (2017) The nuclear matrix protein CIZ1 facilitates localization of Xist RNA to the inactive X-chromosome territory. *Genes Dev* 31:876–888.
34. Smola MJ, et al. (2016) SHAPE reveals transcript-wide interactions, complex structural domains, and protein interactions across the Xist lncRNA in living cells. *Proc Natl Acad Sci USA* 113:10322–10327.
35. Nishibe R, et al. (2013) CIZ1, a p21Cip1/Waf1-interacting protein, functions as a tumor suppressor in vivo. *FEBS Lett* 587:1529–1535.
36. Yildirim E, et al. (2013) Xist RNA is a potent suppressor of hematologic cancer in mice. *Cell* 152:727–742.
37. Mali P, et al. (2013) RNA-guided human genome engineering via Cas9. *Science* 339:823–826.
38. Ran FA, et al. (2013) Genome engineering using the CRISPR-Cas9 system. *Nat Protoc* 8:2281–2308.